

Classification  
 Physics Abstracts  
 02.30 — 03.20

## Period doubling boundaries of a bouncing ball

N. B. Tuffiaro, T. M. Mello, Y. M. Choi and A. M. Albano

Physics Department, Bryn Mawr College, Bryn Mawr, Pennsylvania 19010, U.S.A.

(Reçu le 24 février 1986, accepté le 12 mai 1986)

**Résumé.** — Nous étudions, dans le régime de doublement de période, un système mécanique simple formé d'une balle rebondissante soumise à des chocs répétés par une table vibrante. Nous faisons varier deux paramètres de contrôle (la fréquence et l'amplitude des vibrations de la table) pour découvrir les courbes qui, dans l'espace des paramètres, séparent les orbites périodiques. Les résultats expérimentaux sont en accord avec les calculs faits dans le cadre d'un modèle simple.

**Abstract.** — A simple mechanical system consisting of a bouncing ball subject to repeated impacts with a vibrating table is studied in the period doubling regime. Two control parameters (the table's forcing frequency and amplitude) are varied to discover the curves in parameter space that separate periodic orbits. Experimental results for the period doubling boundaries agree with calculations from a simple model.

### 1. Introduction.

A nonlinear mechanical oscillator consisting of a bouncing ball subject to repeated impacts with a vibrating table is being studied by several research groups who are interested in exploring the chaotic dynamics of simple systems [1-3]. As illustrated in figure 1, the ball is free to bounce inelastically on a table which moves sinusoidally up and down. An experimental apparatus to study the bouncing ball system is easy to construct from a loud speaker, ball bearing, and a function generator [1, 2]. Pierański recently demonstrated that the bouncing ball system exhibits a period doubling instability [2]. Holmes and Pierański, in separate research efforts, both choose to model the bouncing ball system by the «dissipative standard map». As Holmes clearly points out, the dissipative standard map is a good model for the bouncing ball system only in the regime where the overall table displacement is small compared to the total distance travelled by the ball between impacts [3].

In this paper we analyse a more realistic model for the bouncing ball system. The dissipative standard map is easier to analyse than the model adopted in this paper because the standard map provides an explicit expression for the next phase and velocity of the ball's impact. The model analysed here relies on an implicit equation to determine the next impact phase. In spite of this we still obtain simple conditions for the existence and stability of period one orbits.

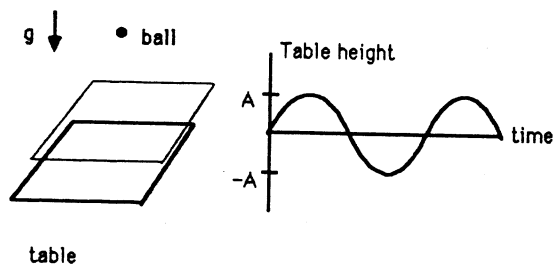


Fig. 1. — Bouncing ball. A ball is free to bounce on a table which moves sinusoidally up and down.

By analysing the period one to period two bifurcation we discover the boundaries in parameter space which separate these two periodic motions. The analysis also allows us to determine the form of boundaries between periodic and chaotic motion when the bouncing ball system undergoes a period doubling cascade.

### 2. Description of model

To model the bouncing ball system we assume that the table's mass is much greater than the ball's mass, and that the impact is instantaneous. Under these conditions, a typical period one orbit is shown in figure 2. The ball's trajectory is determined by specifying the phase of impact (relative to the table's frequency) as well as the velocity of the ball immediately before and after impact.

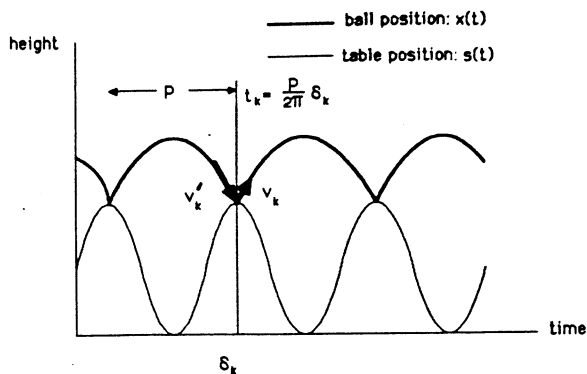


Fig. 2. — Ball and table position. Period motion of period  $P$  is depicted. Prime denotes ingoing velocity.

The change in the ball's velocity at impact is calculated from the usual impact relation [4] :

$$v_k - w_k = -\alpha [v'_k - w_k] \quad (1)$$

where  $0 < \alpha \leq 1$  is the coefficient of restitution (dissipation rate) and  $v'_k$ ,  $v_k$  and  $w_k$  are the absolute velocities of the incoming ball, outgoing ball, and the table at the  $k$ th impact. The system is conservative when  $\alpha = 1$ .

The phase of impact is calculated by considering the difference between the ball and table position. Let

$$x(t) = x_k + v_k(t - t_k) - \frac{1}{2} g(t - t_k)^2 \quad (2)$$

be the ball position after the  $k$ th impact where  $x_k$  is the position at the  $k$ th impact, and  $t_k$  is the time of the  $k$ th impact; and let

$$s(t) = A[\sin(\omega t + \delta) + 1] \quad (3)$$

be the table position with amplitude  $A$ , and angular frequency  $\omega$ , and offset  $\delta$  at  $t = 0$ . The difference in position between the ball and table is

$$d(t) = x(t) - s(t) \quad (4)$$

which is always positive for a small enough  $t$ . The first value of  $t$  for which  $d = 0$  implicitly defines the time (and hence phase) of the next impact.

Elementary considerations of projectile motion allow us to write down the mapping for  $v_{k+1}$  and  $\delta_{k+1}$  in terms of only  $v_k$  and  $\delta_k$ . The mapping for the bouncing ball system, with forcing period  $P$ , consists of an implicit phase map,

$$d(\delta) = A[\sin(\delta_k) + 1] + v_k \left( \frac{P}{2\pi} (\delta - \delta_k) \right) - \frac{1}{2} g \left( \frac{P}{2\pi} (\delta - \delta_k) \right)^2 - A[\sin(\delta) + 1] \quad (5)$$

where  $\delta_{k+1}$  is the next  $\delta$  for which  $d(\delta) = 0$ ; and an

explicit velocity map (from Eq. (1)) :

$$v_{k+1} = (1 + \alpha) \frac{2\pi A}{P} \cos(\delta_{k+1}) - \alpha \left\{ v_k - g \left[ \frac{P}{2\pi} (\delta_{k+1} - \delta_k) \right] \right\} \quad (6)$$

The dynamics of the bouncing ball are easy to simulate on a computer using equations (5) and (6). The only real numerical work is in finding the zeros of the phase function. Examples of computer simulations are shown in figures 3 and 4. Figure 3 shows a stable period two orbit. Figure 4 illustrates part of the trajectory of a chaotic orbit.

### 3. Period one orbits.

For a period one orbit

$$v_k = -v'_k, \quad (7)$$

$$v_k = \frac{gP}{2}. \quad (8)$$

$A = 0.006, f = 80, X_1 = -0.008, V_1 = 6.647, V_{table} = 3.015$   
Damping = 0.5

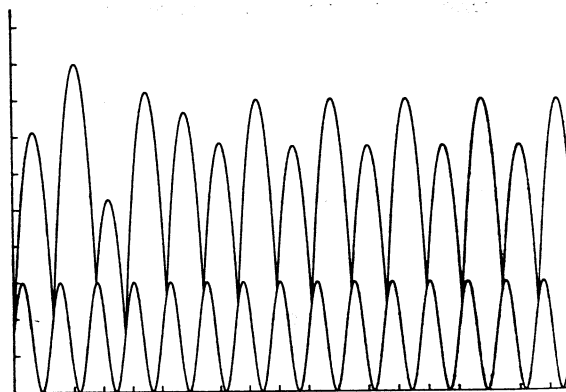


Fig. 3. — Computer simulation of a period two orbit.

$A = 0.007, f = 80, X_1 = 3.18207, V_1 = 3.396, V_{table} = 3.482$   
Damping = 0.5

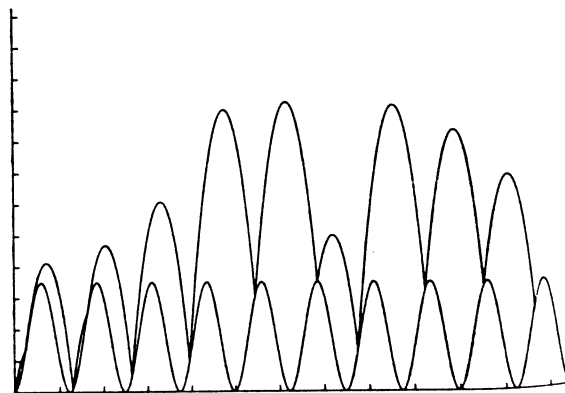


Fig. 4. — Computer simulation showing part of a chaotic orbit.

From equation (1) it follows that a necessary and sufficient condition for the existence of a period one orbit is

$$\cos(\delta) = \frac{gP^2}{4\pi A} \left( \frac{1-\alpha}{1+\alpha} \right). \quad (9)$$

Equation (9) specifies two separate periodic orbits, only one of which is usually stable. In the conservative limit ( $\alpha = 1$ ) the unstable (hyperbolic fixed point) orbit usually occurs at  $\delta = -\pi/2$  while the stable orbit (elliptic fixed point) is at  $\delta = \pi/2$ . For a given forcing frequency and amplitude, equations (8) and (9) specify the phase and initial velocity needed to obtain a period one orbit. However these relations give no hint as to the stability of a periodic orbit.

In a period doubling cascade the period one orbit gives birth to a stable period two orbit exactly when the period one orbit becomes unstable. The period doubling bifurcation is also referred to as a « flip bifurcation » because the iterates of the map hop from side to side as they approach (or depart) the fixed point [5]. The eigenvalues of the map (linearized about the fixed point) determine the stability of an orbit. If the absolute value of both eigenvalues is less than one then the orbit is stable. The orbit becomes unstable as soon as the absolute value of one of the eigenvalues is greater than one. For a flip bifurcation the eigenvalues are in fact negative. Therefore a periodic orbit becomes unstable (or stable) precisely when one of the eigenvalues equals  $-1$ .

In order to linearize the bouncing ball map about a period one orbit we need to calculate (to first order) how much a small perturbation of the velocity and phase affects a subsequent impact. From figure 5 we find the following relationships among  $\delta_1$ ,  $\delta_2$ ,  $v_1$ , and  $v_2$  :

$$A \sin(\delta_2) = A \sin(\delta_1) + v_1 \frac{(\delta_2 - \delta_1)}{\omega} - \frac{1}{2} g \left( \frac{\delta_2 - \delta_1}{\omega} \right)^2 \quad (10)$$

and

$$v_2 = (1 + \alpha) \omega A \cos(\delta_2) - \alpha \left[ v_1 - g \frac{(\delta_2 - \delta_1)}{\omega} \right] \quad (11)$$

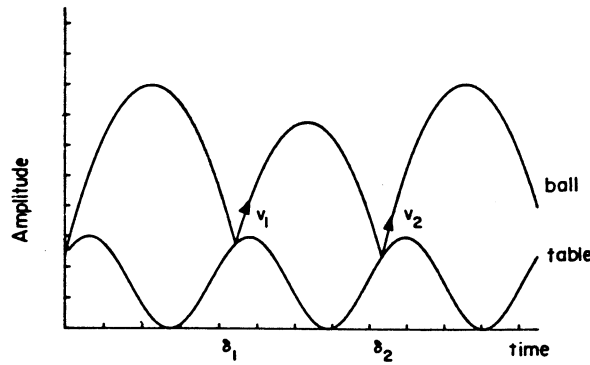


Fig. 5. — Ball and table position from numerical simulation. The phase and velocity variables are related by elementary considerations of projectile motion. The numerical simulation shows that the phase of impact can not be neglected when computing the time of flight between impacts.

where  $\omega = 2\pi/P$ . Equation (10) simply equates the position of both the ball and the table at  $\delta_1$  and  $\delta_2$  while equation (11) relates the velocities.

Near a period one orbit we have

$$\delta_1 = \delta_{p1} + 2\pi\epsilon_1 \quad (12)$$

$$\delta_2 = \delta_{p1} + 2\pi(1 + \epsilon_2) \quad (13)$$

$$v_k = v_{p1}(1 + \eta_k); \quad (k = 1, 2), \quad (14)$$

where  $\delta_{p1}$  and  $v_{p1}$  denote the phase and velocity at impact of a period one orbit as specified by equations (8) and (9);  $\epsilon_k$  and  $\eta_k$  represent a small perturbation in both the phase and velocity. Substituting equations (12-14) in (10) and keeping only terms of first order yields

$$\epsilon_2 = \epsilon_1 + \left( \frac{1 + \alpha}{2} \right) \eta_1 \quad (15)$$

while equation (11) results in,

$$\eta_2 = [-2\pi(1 - \alpha) \tan(\delta_{p1})] \epsilon_1 + [\alpha^2 - \pi(1 - \alpha^2) \tan(\delta_{p1})] \eta_1. \quad (16)$$

This linearized map is expressed more neatly by the matrix :

$$\begin{pmatrix} \epsilon_2 \\ \eta_2 \end{pmatrix} = \begin{pmatrix} 1 & \frac{1 + \alpha}{2} \\ -2\pi(1 - \alpha) \tan(\delta_{p1}) & \alpha^2 - \pi(1 - \alpha^2) \tan(\delta_{p1}) \end{pmatrix} \begin{pmatrix} \epsilon_1 \\ \eta_1 \end{pmatrix} \quad (17)$$

which we will call  $Df$ . The determinant of  $Df$ ,  $\det(Df) = \alpha^2$ , which says that the phase space contracts when

$\alpha < 1$ . The conservative case ( $\alpha = 1$ ) preserves area in phase space.

With  $Df$  we can calculate the stability of a period one orbit. The two eigenvalues of  $Df$  are

$$\lambda_{\pm} = \frac{-b \pm \sqrt{b^2 - 4\alpha^2}}{2}, \quad (18)$$

$$b = \pi(1 - \alpha^2) \tan(\delta) - (1 + \alpha^2). \quad (19)$$

To find the value at which a period one to period two transition takes place we set  $\lambda_{\pm} = -1$  (for a flip bifurcation) which implies

$$\tan(\delta_{\text{bif}}) = \frac{2}{\pi} \left( \frac{1 + \alpha^2}{1 - \alpha^2} \right). \quad (20)$$

Equation (20) has a number of interesting implications. First, it states that the phase at which a period one to period two bifurcation takes place depends only on the coefficient of restitution and is therefore constant for a fixed experimental system. Second, the phase of bifurcation is easy to obtain from the experimental apparatus so equation (20) provides a measurement of the coefficient of restitution [1]. Third, the fact that  $\delta_{\text{bif}}$  is constant allows us to determine the curves in parameter space (forcing amplitude and frequency) that separate the period one to period two transition. Since equation (9) holds for any period one motion; it follows that

$$A = \frac{g}{4\pi \cos(\delta_{\text{bif}})} \left( \frac{1 - \alpha}{1 + \alpha} \right) P^2. \quad (21)$$

Therefore, a graph of  $A$  vs.  $P^2$  at the period one to period two transition should result in a linear plot.

**4. Experimental results.**

Both numerical simulations and experiments with a bouncing ball apparatus constructed from a loud speaker and a ball bearing are employed to check the results of section 3. In both cases we vary the forcing frequency and amplitude (the coefficient of restitution is constant) to discover where in parameter space a period one to period two transition occurs. In addition, data is presented for the higher order period doubling transitions. Following equation (21) we plot  $A$  vs.  $P^2$  for all the period doubling transitions.

The results from numerical simulations are presented in figure 6. Of course, the results agree exactly with equation (21) for the period one to period two transition. Somewhat surprisingly, however, the boundaries between the higher period doubling transitions are also linear when we plot  $A$  vs.  $P^2$ . This result can be explained by writing the impact map in dimensionless variables and noting that the ratio  $A/P^2$  is a fixed constant at any period doubling bifurcation [6].

An experimental realization of the bouncing ball system is depicted in figure 7. A speaker, driven by a function generator, serves as the vibrating table. A small ball bounces on a concave lens glued to the

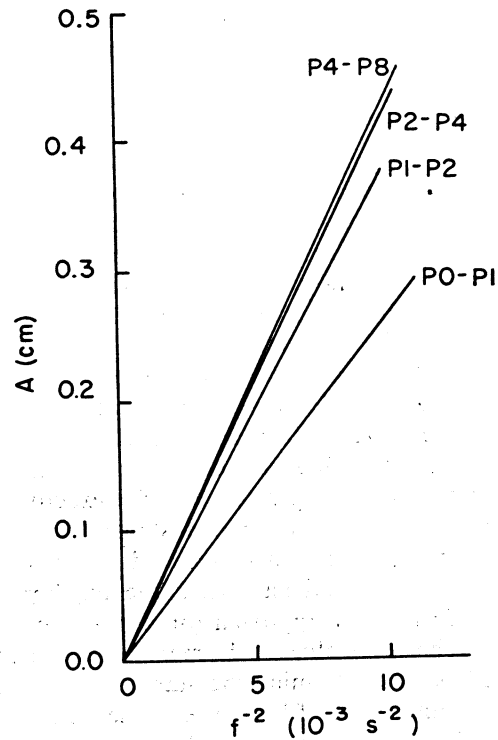


Fig. 6. — Period doubling boundaries calculated from numerical simulations ( $\alpha = 0.5$ ). All the boundaries appear linear when we plot the table amplitude,  $A$  vs. the period squared.

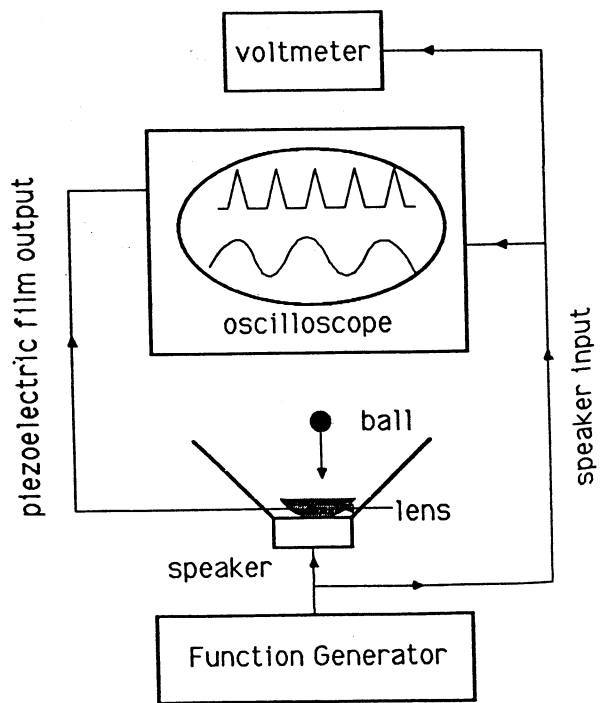


Fig. 7. — Apparatus for the bouncing ball experiment. A thin piezoelectric film mounted to the surface of the lens detects an impact between the ball and the lens.

speaker - ball's mc lens is a voltage s voltage s period d read fr non gene the table micro-po speaker s impacts the piezo positione between ly deter on and j frequency bifurcatic Results the given simulation ent of th for the system period for truncati erent v presen the perio suggested

**Conclu**

We analy the bo boundarie in perio that the j period tw resitut tion ph efficient Our res period on tion a

speaker — the curvature of the lens helps to keep the ball's motion vertical. Fastened to the surface of the lens is a thin ( $28 \mu$ ) piezoelectric film that generates a voltage spike every time the ball hits the lens. The voltage spike is monitored on an oscilloscope to detect period doubling bifurcations. The forcing frequency is read from a frequency meter connected to the function generator. In order to measure the amplitude of the table's oscillation, a bit more care is required. A micro-positioner is mounted across the top of the speaker so that the tip of the micro-positioner lightly impacts with the lens (the impacts are detected by the piezoelectric film). By gently sliding the micro-positioner vertically, and looking for the initial impact between the tip and the lens, it is possible to accurately determine the table's actual amplitude of oscillation and phase. In this way we can measure the table's frequency, amplitude, and phase at a period doubling bifurcation.

Results from the experimental bouncing ball system are given in figure 8. The agreement with the numerical simulations is excellent. An experimental measurement of the phase of bifurcation yields approximately 0.5 for the coefficient of restitution. In the experimental system it is not possible to obtain orbits higher than period four without the system exhibiting chaos. This «truncation of the cascade» is the effect of noise inherent within the mechanical apparatus and is not, at present, accounted for in the numerical model. The period four to chaos boundary is indeed linear as suggested by the numerical simulations.

## 5. Conclusion.

We analysed the period one to period two transition in the bouncing ball system. The analysis yields the boundaries, in parameter space, which separate different periodic and chaotic motions. We also discovered that the phase of bifurcation for the period one to period two transition depends only on the coefficient of restitution; and hence, a measurement of the bifurcation phase provides a simple determination of the coefficient of restitution.

Our results also suggest that a simple analysis of the period one to period two transition may yield information about the boundaries, in parameter space,

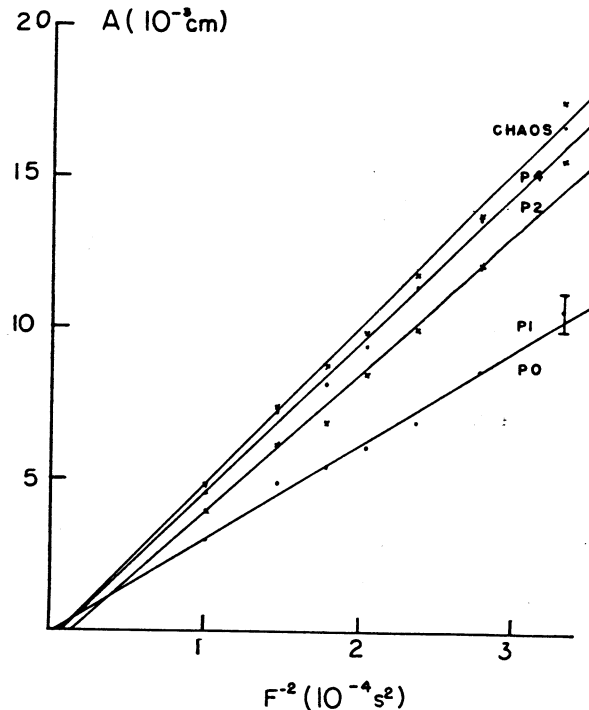


Fig. 8. — Experimental results for the period doubling boundaries from a bouncing ball apparatus. The boundaries show good agreement with numerical simulations. The amplitude is measured with a micrometer.

separating periodic and chaotic motion. We also suspect that many forced and dissipative dynamical systems may be similar to the bouncing ball system in that the phase at which a period doubling bifurcation takes place depends only on a single parameter, the dissipation rate. An analysis, then, of the period one to period two transition may prove to be a useful heuristic guide in determining the boundaries of chaotic motion in systems exhibiting period doubling instabilities.

## Acknowledgments.

We thank K. Hartnett, N. Abraham, G. Alman, and D. Griffiths for their encouragement and technical support. We also thank D. Pine for the loan of a signal generator.

## References

- [1] TUFILLARO, N. B. and ALBANO, A. M., *Am. J. Physics* (to appear); MELLO, T. M. and TUFILLARO, N. B., Strange attractors of a bouncing ball, *Am. J. Physics* (to appear).
- [2] PIERAŃSKI, P., *J. Physique* **44** (1983) 573-578; FRANSZEK, M. and PIERAŃSKI, P., *Can. J. Phys.* **63** (1985) 488; PIERAŃSKI, P., KOWALIK, Z. and FRANSZEK, M., *J. Physique* **46** (1985) 681-686; PIERAŃSKI, P. and BARTOLINO, R., *J. Physique* **46** (1985) 687.
- [3] HOLMES, P. J., The dynamics of repeated impacts with a sinusoidally vibrating table, *J. Sound Vib.* **84** (1982) 173-189.
- [4] MERIAM, J. L., *Dynamics* (Wiley, New York) 1975.
- [5] GUCKENHEIMER, J. and HOLMES, P., *Nonlinear Oscillations, Dynamical Systems, and Bifurcations of Vector Fields* (Springer-Verlag, New York) 1983, p. 102-116.
- [6] WIESENFELD, K. and HOLMES, P., pointed out to us that the ratio of  $A/P^2$  is constant for all the period doubling boundaries because of simple dimensionality considerations.

Classificati  
Physics A  
34.00 —

Section  
Transi

Introdu

Etude d  
lignes él  
rsonance  
s jets m  
certa  
éta  
jet m  
œuvre  
occur  
lectar  
tra  
transi  
de av  
sure  
propr  
transi  
K' d  
le  
men  
l'é  
du  
mbre  
ollisic